

Development of a Neural Network-Based Fault Diagnostic System

Soteris Kalogirou¹, Georgios Florides¹, Sylvain Lalot², Bernard Desmet²

1. Higher Technical Institute, P.O.Box 20423, Nicosia 2152, Cyprus

2. University of Valenciennes and Hainaut-Cambresis, Le Mont Houy, 59313 Valenciennes Cedex 9, France

ABSTRACT

The objective of this work is to present the development of an automatic solar water heater (SWH) fault diagnosis system (FDS). The FDS system consists of a prediction module, a residual calculator and the diagnosis module. A data acquisition system measures the temperatures at four locations of the SWH system. In the prediction module an artificial neural network (ANN) is used, trained with values obtained from a TRNSYS model of a fault-free system operated with the typical meteorological year (TMY) files of Nicosia, Cyprus and Paris, France. Thus, the neural network is able to predict the fault-free temperatures under different environmental conditions. The input data to the ANN are the time of the year, various weather parameters and one input temperature. The residual calculator receives both the current measurement data from the data acquisition system and the fault-free predictions from the prediction module. The system can predict three types of faults; collector faults and faults in insulation of the pipes connecting the collector with the storage tank and these are indicated with suitable labels. The system was validated by using input values representing various faults of the system.

Keywords: Fault diagnostic system, artificial neural networks, solar water heating systems

1. INTRODUCTION

Solar water heating (SWH) systems are not usually equipped with any fault diagnostic system (FDS). Any faults are usually identified either by regular inspection by servicing personnel or when the system is not producing appropriate quantities of hot water, which is the most frequent. Usually people forget the existence of the solar system and this is inspected only after hot water is not available, indicating some problems. This results in problematic operation of the systems for long periods of time, which reduce the effectiveness and viability of the systems.

2. DESCRIPTION OF SOLAR SYSTEM

The solar system considered in this work is a large hot water one suitable for a small hotel, blocks of flats, offices or similar applications. Although the FDS system developed can be applied to small systems as well it is thought that the expenditure required would not balance the extra benefits incurred in such cases and in domestic applications the users are usually

more sensitive to the maintenance of their own system in comparison with the maintenance staff of a hotel for example or the tenants of a multi building installation where everybody but really nobody is responsible. The system diagrammatic is shown in Fig. 1. The system consists of 40m² of collectors, a differential thermostat (not shown in Fig. 1) and a 2000 liters storage tank. The system is also equipped with a data acquisition system which measures the temperatures at four locations of the SWH system; the collector outlet (T₁), the storage tank inlet (T₂), the storage tank outlet (T₃) and the collector inlet (T₄).

A TRNSYS model of the system predicts the four temperatures of a fault-free system operated with the typical meteorological year (TMY) files of Nicosia, Cyprus and Paris, France. It should be noted that the actual performance characteristics of a real system were used in TRNSYS. The data obtained from TRNSYS were used to train a number of artificial neural networks (ANNs). In an actual system, real fault-free data collected for a certain period of time can be used for training.

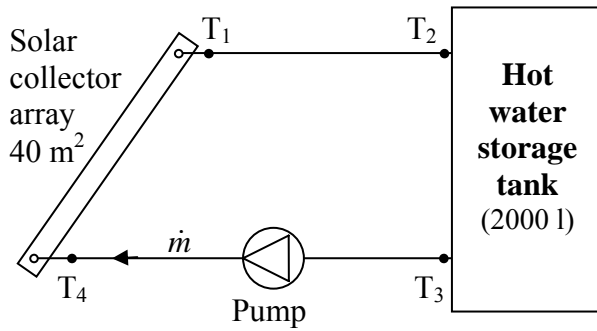


Fig. 1 Schematic diagram of the simple solar system

3. ANN MODELS

Six ANNs, one for each temperature (T_1 , T_2 and T_4) for each location, were trained to predict the required temperatures. The objective is to compare the ANNs predicted temperatures against measured temperatures from the data acquisition system and from any differences between the two to decide whether the system has any fault or if it is working normally. The neural networks are of the multiple perceptron type with three hidden layers; each with a different activation function, see [1-3] for details. For the training of the ANNs the TRNSYS results of a “fault-free” system were used. For Cyprus, 4377 data were available (sunshine data only) from which 3282 were used for the training and 1095 for the validation of the ANNs. Similarly, for France, 4364 data were available in total, from which 3273 were used for the training and 1091 for the validation of the ANN. Thus, the neural network is able to predict the fault-free temperatures under different environmental conditions. The ratio of the validation set size to the training set size is much higher than the one suggested in [4].

The input data to the ANN are the time of the year (from 1 to 8760), global solar radiation on a horizontal surface, beam radiation, ambient temperature, incidence angle, wind speed, relative humidity, flow availability (0 for no flow or 1 for flow) and input temperature (T_{in}) according to the case, i.e., for the prediction of T_1 temperature T_4 was used as input, for T_2 temperature T_1 is used as input and for T_4 temperature T_3 is used as input. In the work presented here, T_3 is not predicted, as this would require the mean storage tank

temperature as an input. A single output is used representing the predicted temperature. A schematic diagram of the ANNs is shown in Fig. 2. It should be noted that a different ANN is used for each temperature and each location.

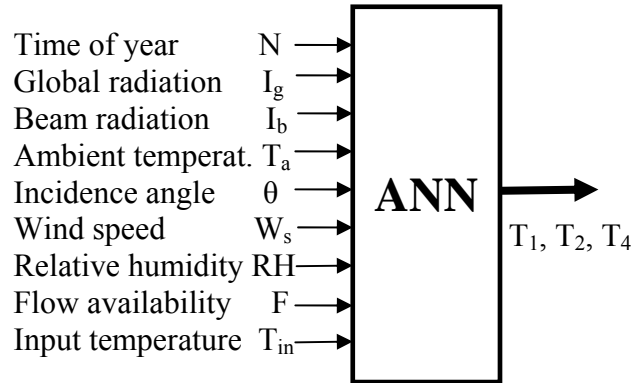


Fig. 2 ANN design concept

The results for the training and validation of the six ANNs are shown in Table 1. In all cases the results are considered as satisfactory. Even in the case of T_2 where low R^2 values were obtained, the ANN predictions were more than 5% of the accepted value for no more than 4 consecutive cases.

Table 1. Coefficient of multiple determination (R^2) for the training and validation of the ANNs

ANN	Country	Prediction	Training	Validation
ANN-1	Cyprus	T_1	0.9998	0.9996
ANN-2		T_2	0.9447	0.8823
ANN-4		T_4	0.9968	0.9920
ANN-5	France	T_1	0.9998	0.9995
ANN-6		T_2	0.9296	0.8258
ANN-8		T_4	0.9912	0.9661

4. FAULT FINDING SYSTEM

The concept of the fault finding system (FDS) is shown schematically in Fig. 3. In the prediction module the trained ANN modules were used to predict the required temperature. The residual calculator receives both the current measurement data from the data acquisition system and the fault-free predictions from the prediction module. The set of residuals r_{col} , r_{U12} and r_{U34} (see section 4.1, below), or differences between the current conditions of parameters and those predicted for fault-free operation (estimated by the ANN), are generated by this module.

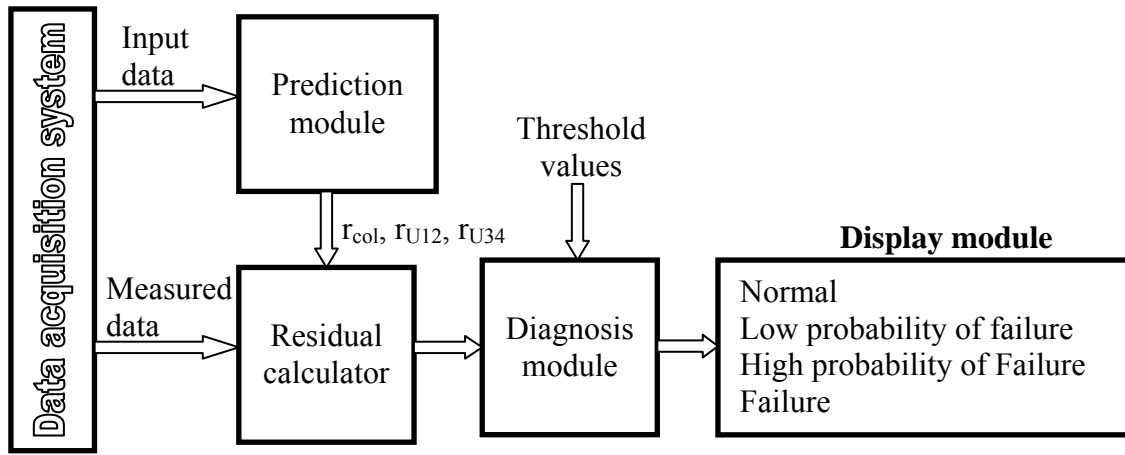


Fig. 3 Concept of the simple FDS

In the diagnosis module the residuals are compared against three constant threshold values. So, four categories are defined: normal, low probability of failure, high probability of failure, and failure. The system can predict three types of faults; collector faults and faults in insulation of the pipes connecting the collector with the storage tank and these are indicated with suitable labels. It cannot however, identify the exact cause of the fault in the solar collector which can be due to dust deposited on the collector glazing, fouling in the collector or problems related to the collector insulation.

4.1 The residual calculator

As already mentioned, the residual calculator receives both the current measurement data from the data acquisition system and the fault-free predictions from the prediction module. The latter are the values predicted by the neural networks presented above. In fact, the residuals are computed only if the pump is on.

Two kinds of residuals are computed. The first is the absolute value of the relative error between the actual and the predicted difference of two temperatures and is used to monitor the condition of the collectors. This residual is given by Eq. (1) where the actual temperature increase $T_{1a}-T_{4a}$ is compared against the predicted temperature increase $T_{1p}-T_{4a}$.

$$r_{col} = \left| \frac{(T_{1a} - T_{4a}) - (T_{1p} - T_{4a})}{T_{1a} - T_{4a}} \right| = \left| \frac{T_{1a} - T_{1p}}{T_{1a} - T_{4a}} \right| \quad (1)$$

The second kind of residuals is the relative error of a temperature difference. It is used for monitoring the conditions of the connecting pipes between the collectors and the storage:

$$r_{U12} = \left| \frac{(T_{1a} - T_{2a}) - (T_{1a} - T_{2p})}{T_{1a}} \right| = \left| \frac{T_{2a} - T_{2p}}{T_{1a}} \right| \quad (2)$$

$$r_{U34} = \left| \frac{(T_{3a} - T_{4a}) - (T_{3a} - T_{4p})}{T_{3a}} \right| = \left| \frac{T_{4a} - T_{4p}}{T_{3a}} \right| \quad (3)$$

4.2 The diagnosis module

The residuals are compared against four categories of faults; normal, low probability of failure, high probability of failure and failure. Each state of the system is decided from the magnitude of the residual, which classifies it to one of each category.

To do so, three thresholds are determined. They depend on the quality of the predictions and the actual state of the system. When the neural networks are accurate and the system is operating without any fault, the thresholds are very low. When each measurement is received, the procedure described in Fig. 4 is applied. As can be seen in Fig. 4, five consecutive residuals are required in each category to determine the state of the system. This is used to avoid false indications or false alarms (in the case of failure of a sub-system) from possible wrong predictions from an ANN or wrong measurements from the data acquisition system, which often occur when there is noise in measurements.

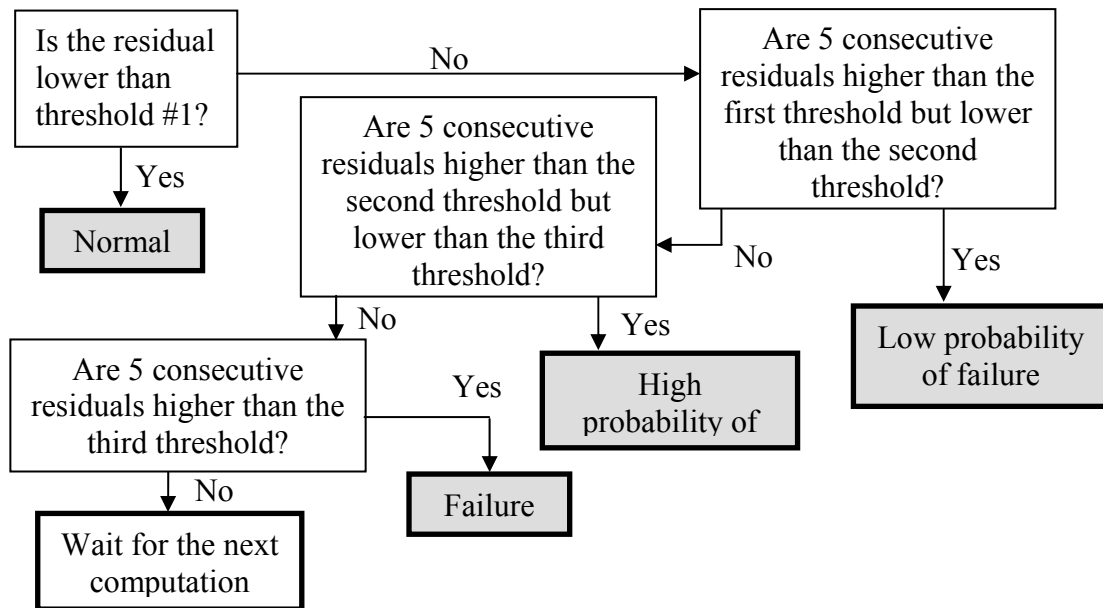


Fig. 4 Procedure applied by the diagnosis module

5. APPLICATION OF THE FDS

The following experiments have been carried out using TRNSYS. The first one concerns the Cypriot solar system. Starting March 1st, the F' coefficient has been progressively decreased from 0.69 to 0.63 (10% decrease compared to the value taken into account during the training process of the neural networks) in seven weeks (0.69 the first week, 0.68 the second week and so on). Figure 5 shows the residuals r_{col} .

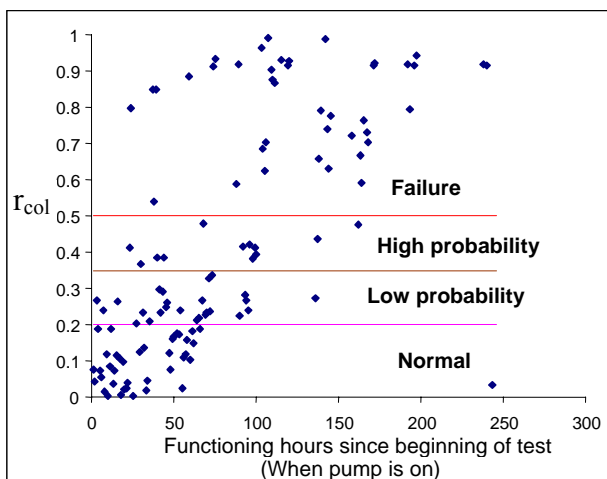


Fig. 5 Plot of r_{col} residuals against functioning hour-Cypriot system

The F' coefficient, i.e., the collector efficiency factor, which represents for a drop of the collector efficiency and accounts for various faults, i.e., deterioration of collector insulation,

fouling of the collector pipes, breaking of collector glazing, alteration in fluid flow rate, separation of riser pipes from the absorbing plates, etc.

Then using 0.2, 0.35, and 0.5 as the three thresholds of the diagnosis module, the "raw" sequence shown in Fig. 6, is obtained.

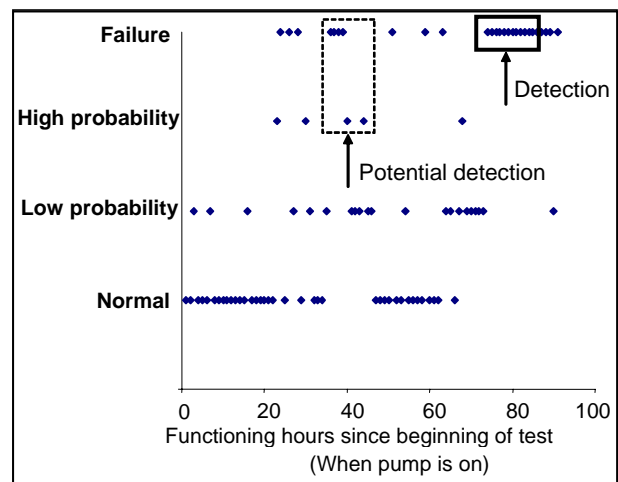


Fig. 6 Plot of the raw sequence against the functioning hour for the collector condition [Cypriot system]

Taking into account the functioning periods (when pump is on), the detection of the failure happens during the 78th hour when F' is 0.67. This represents a 5% decrease of the normal value. Note that taking a decision when 5 consecutive readings of either failure, low or

high probability of failure occur would have lead to the detection when F' is 0.68.

The second experiment concerns the French system. The procedure is identical to the one presented for the Cypriot system, except that the starting date is June 1st.

The analysis of the raw sequence (Fig. 7) of “normal”, “low probability”, “high probability” and “failure” leads to the detection of the failure during the 76th functioning hour, when F' is 0.67. Note that the thresholds are equal to the thresholds used for the analysis of the Cypriot system.

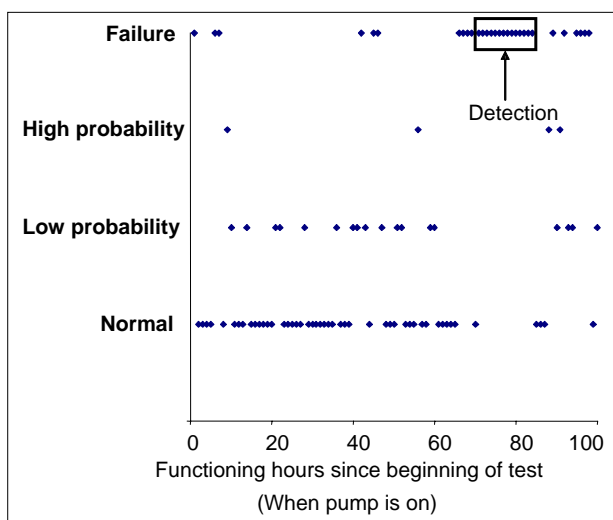


Fig. 7 Plot of the raw sequence against the functioning hour for the collector condition [French system]

Similar experiments have been carried out for the prediction of the deterioration of insulation of the connecting pipes. For the first one, an increase (by 10%) of the U value of the pipe connecting the outlet of the collectors to the storage (circuit 1-2) is simulated for the French system starting on July 1st. The analysis is carried out on the temperature difference between T_1 and T_2 when the pump is running. As already mentioned, the actual value of T_1 is considered and the predicted value of T_2 is used to compute the relative error. This makes the detection independent of a possible deterioration of the efficiency of the collectors. The detection of this failure during the 96th functioning hour (see Fig. 8) corresponds to about a 5% increase of the U value, when 0.01, 0.015, and 0.02 are the three thresholds.

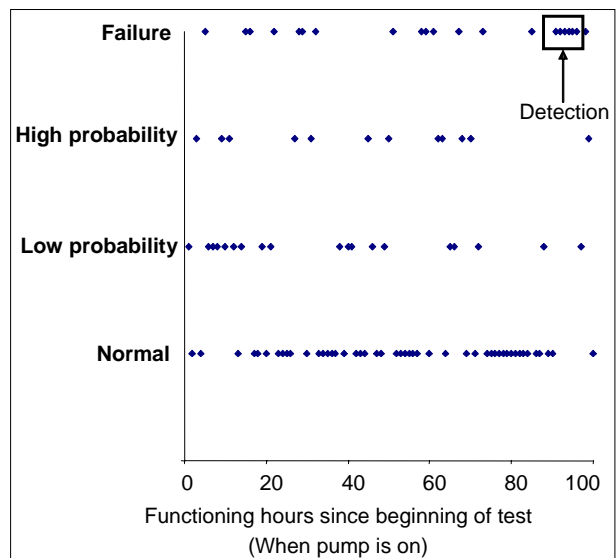


Fig. 8 Plot of the raw sequence against the functioning hour for circuit 1-2 (r_{U12} residuals) [French system]

The last experiment concerns the U value for the connecting pipe between the storage and the inlet of the collectors (circuit 3-4). The experiment begins on March 1st for the Cypriot system. Once again the analysis of the states sequence leads to the detection of the failure of the insulation when a 5% increase of the U value is observed (during the 69th functioning hour). Figure 9 shows the residuals versus the functioning time whereas Fig. 10 shows the corresponding sequence used for detection. In this case, the thresholds have to be adjusted to 0.04, 0.06, and 0.08. It should be noted that due to lack of space only one circuit is presented for each location.

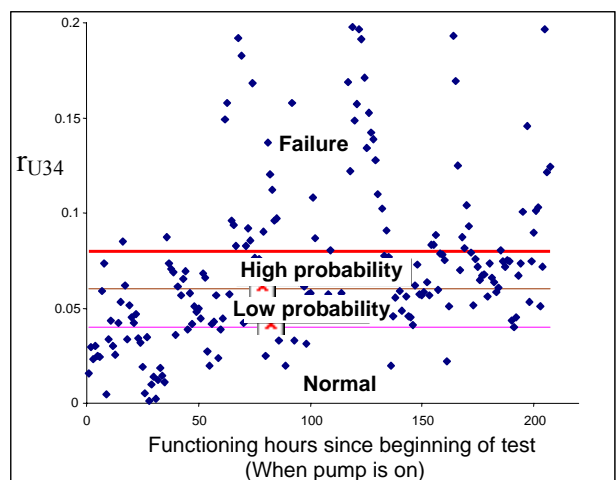


Fig. 9 Plot of r_{U34} residuals against functioning hour-Cypriot system

As can be seen, the residuals are not continuously increasing. Therefore, for other more complex systems, systems located in other regions/countries, or maybe larger or smaller systems, the residuals would not evolve as they do here therefore it could be necessary to use a more complex monitoring tool such as the one presented in [5] or its derivative version presented in [6, 7].

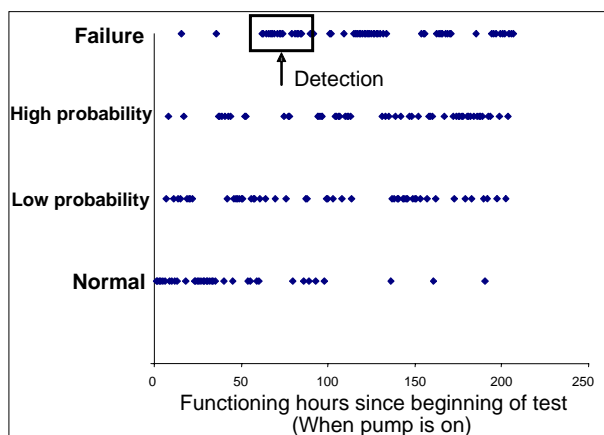


Fig. 10 Plot of the raw sequence against the functioning hour for circuit 3-4 (r_{U34} residuals) [Cypriot system]

6. CONCLUSIONS

In this paper, the design of a solar system fault diagnostic system is presented. The system consists of a prediction module, a residual calculator and the diagnosis module. A data acquisition system measures the temperatures at four locations of the SWH system. In the prediction module an ANN is used, trained with values obtained from a TRNSYS model of a fault-free system for Nicosia and Paris. Thus, the neural network is able to predict the fault-free temperatures under different environmental conditions. The input data to the ANN are the time of the year, various weather parameters and one input temperature. The residual calculator receives both the current measurement data from the data acquisition system and the fault-free predictions from the prediction module. The system can predict three types of faults; collector faults and faults in insulation of the pipes connecting the collector with the storage tank.

The system was validated by using input values representing various faults of the system. In all

cases, the faulty operation was predicted satisfactorily. In a future research, we are planning to develop a system, which will be able to identify the exact cause of each fault.

It is believed by the authors that solar FDS can increase the reliability of the systems and thus the economic benefits resulting by their use.

ACKNOWLEDGEMENTS

The financial support of the French Ministry of Foreign Affairs (under contract EGIDE 11999SD) and of the Cyprus Research Foundation (under contract KY-ΓA/0305/02) is greatly acknowledged.

REFERENCES

- [1] Kalogirou S. A., Neocleous C. C., Schizaz C. N., 1998. Artificial neural networks for modeling the starting-up of a solar steam-generator, *Applied Energy*, Vol. 60, No. 2, pp. 89-100.
- [2] Kalogirou S. A., Panteliou S., 2000. Thermosiphon solar domestic water heating systems: long-term performance prediction using artificial neural networks, *Solar Energy*, Vol. 69, No. 2, pp. 163-174.
- [3] Kalogirou S. A., 2006. Prediction of flat-plate collector performance parameters using artificial neural networks, *Solar Energy*, Vol. 80, No. 3, pp. 248-259.
- [4] S. Haykin, 1999, *Neural networks- a comprehensive foundation*, Prentice Hall, Upper Saddle River, New Jersey.
- [5] S. Lecoeuche, C. Lurette, S. Lalot, 2004, New supervision architecture based on on-line modelling of non-stationary data, *Neural Computing and Applications*, Vol. 13 No. 4, pp 323-338.
- [6] S. Lalot, 2006, On-line detection of fouling in a water circulating temperature controller (WCTC) used in injection moulding, Part 1: Principles, *Applied Thermal Engineering*, Vol. 26, No. 11-12, pp. 1087-1094.
- [7] S. Lalot, 2006, On-line detection of fouling in a water circulating temperature controller (WCTC) used in injection moulding, Part 2: Application, *Applied Thermal Engineering*, Vol. 26, No. 11-12, pp. 1095-1105.